ARTICLES
PUBLISHED ONLINE: 15 MAY 2011 | DOI: 10.1038/NMAT3026

nature materials

Tailoring organic heterojunction interfaces in bilayer polymer photovoltaic devices

Akira Tada[1], Yanfang Geng[1,2], Qingshuo Wei[3], Kazuhito Hashimoto[1,3]★ and Keisuke Tajima[1,3]★

In an ideal model, a p–n junction is formed by two stacked slabs of semiconductors. Although the construction of actual devices is generally more complex, we show that such a simple method can in fact be applied to the formation of organic heterojunctions. Two films of the organic semiconductors poly(3-hexylthiophene) (P3HT) and [6,6]-phenyl-C_{61}-butyric acid methyl ester (PCBM) can be connected by a simple film-transfer method without disturbing their flat surfaces. Each film can further be modified with a surface-segregated monolayer to tune the strength and direction of the surface dipole moment. Using this method, we fabricated bilayer organic photovoltaic devices with interfacial dipole moments that were selected to align the energy levels at the heterojunction. The open-circuit voltages of the P3HT/PCBM devices could be tuned over a wide range between 0.3 and 0.95 V, indicating that, even if the same combination of bulk materials is used, the interfacial properties drastically alter the performance of organic photovoltaic devices.

The interfacial properties of organic semiconducting materials are important to ascertain the working mechanisms of organic electronic devices such as organic photovoltaic devices (OPVs), as well as to improve their performance[1,2]. In particular, control of electronic properties such as the energy levels of the highest occupied and lowest unoccupied molecular orbitals (HOMO and LUMO) is critical to induce efficient charge separation and to obtain a high open-circuit voltage (V_{OC}) in OPVs. When organic semiconductors are photoirradiated, bound electron–hole pairs (excitons) are generated in the molecules, and these excitons dissociate into free charges only at material interfaces driven by the energy offset, resulting in photocurrent generation[3]. As reported by researchers who have studied many different material combinations, the maximum V_{OC} attainable in OPVs is associated with the energy difference between the LUMO of the acceptor and the HOMO of the donor at the interface (ΔE_{HL} in Fig. 1a; refs 4–7). However, the electronic structure at an interface could strongly depend on how the materials make contact with each other, which in turn is governed by many factors such as interfacial dipole moments induced by the molecular orientation and electronic coupling of the materials. Accordingly, it is necessary to investigate how the properties of organic/organic interfaces influence device performance under conditions that more closely resemble those of an actual device.

Organic/organic interfaces formed by wet processes, however, are extremely difficult to fabricate and to analyse by conventional techniques. Recently, several stamping or lamination methods[8–14] have been developed for forming organic bilayer structures. However, in most cases, heat and pressure are applied to transfer the films, which can also induce material mixing and molecular disordering at the interface. Therefore, to fabricate well-defined organic heterointerfaces, as well as to find the relation between their structure and device performance, methods are needed that can preserve surface structures.

Recently, we have developed a contact film-transfer (CFT) method[15–17]. With this method, one organic layer can be easily stacked, upside down, onto another organic layer under mild conditions. The CFT can be carried out without heat or external pressure, which enables flat and well-defined material interfaces where the structure of each surface is preserved. Furthermore, this method enables analysis and modification of each surface before construction of the organic/organic interface. We have reported the fabrication by this method of organic thin-film transistors with high carrier mobility along the interface owing to the well-ordered 'edge-on' structure of the conjugated polymer surfaces[18].

In this work, we first demonstrated that charge separation and charge transport in OPVs could successfully take place across the organic interfaces fabricated by the CFT method. Next, we modified each surface of the donor and acceptor films with a surface-segregated monolayer (SSM) of fluorinated compounds, and characterized the surface energy structure by ultraviolet photoelectron spectroscopy (UPS). The same surfaces were then brought into contact by the CFT method, and well-defined organic/organic interfaces were prepared for OPVs. Finally, we investigated the correlation between the V_{OC} values of the resulting bilayer OPVs and their interfacial dipole moments measured before device fabrication.

Bilayer OPVs with the structure indium tin oxide (ITO)/TiO_2/[6,6]-phenyl-C_{61}-butyric acid methyl ester (PCBM in Fig. 2a)//poly(3-hexylthiophene) (P3HT in Fig. 2b)/V_2O_5/Al were fabricated by transferring a P3HT layer onto an ITO/TiO_2/PCBM film by the CFT method and then depositing V_2O_5 and Al under vacuum, where // denotes the interface formed by CFT. Details of the methods for device fabrication and characterization are provided in the Methods section. The PCBM and P3HT layers were 45 and 40 nm in thickness, respectively. The current density–voltage (J–V) characteristics of the as-prepared device are shown in Fig. 3a. The bilayer devices showed clear photovoltaic characteristics with V_{OC} of 0.50 ± 0.03 V, a short-circuit current density (J_{SC}) of 1.51 ± 0.11 mA cm^{-2} and a fill factor (FF) of 0.53 ± 0.06, resulting in a power conversion efficiency (PCE) of $0.40 \pm 0.07\%$ (Table 1). This result indicates that the PCBM//P3HT interface formed by

---

[1]Department of Applied Chemistry, School of Engineering, The University of Tokyo, 7-3-1 Hongo, Bunkyo-ku, Tokyo 113-8656, Japan, [2]Department of Materials, School of Materials, Beijing Institute of Technology, 5 South Zhongguancun Street, Haidian District, Beijing 100081, China, [3]HASHIMOTO Light Energy Conversion Project, Exploratory Research for Advanced Technology (ERATO), Japan Science and Technology Agency (JST), Japan.
*e-mail: hashimoto@light.t.u-tokyo.ac.jp; k-tajima@light.t.u-tokyo.ac.jp.

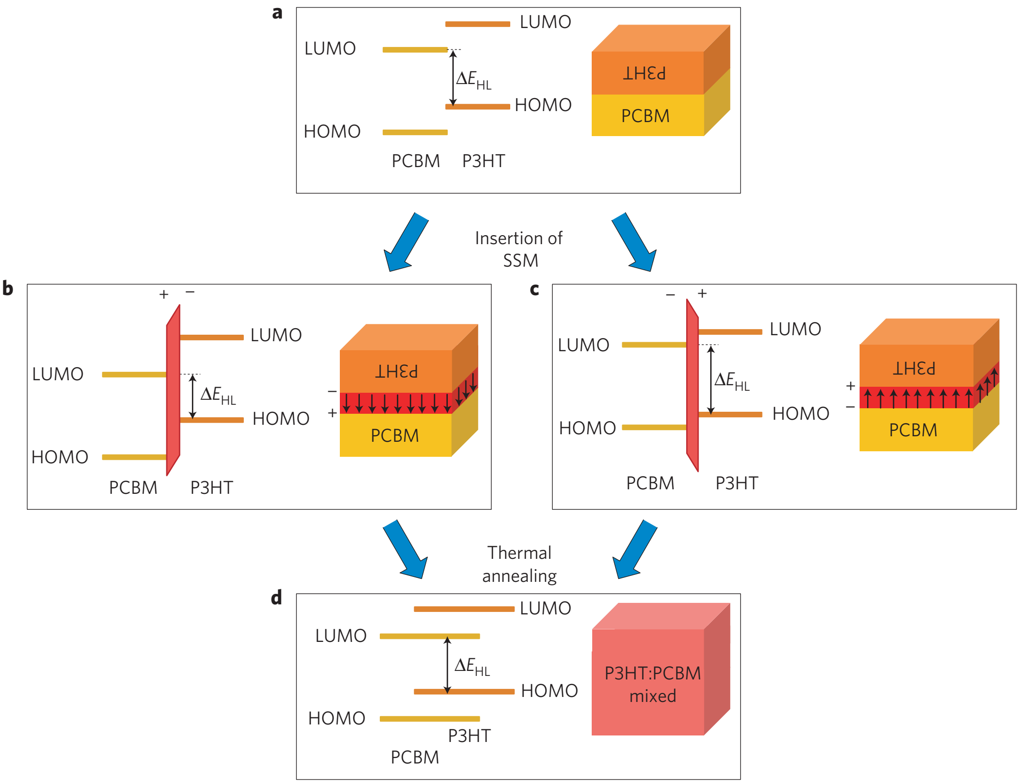

Figure 1 | Schematic representation and energy diagrams of the P3HT/PCBM bilayer devices. a, Without interfacial dipole moments. **b**, With interfacial dipole moments of FC_8. **c**, With interfacial dipole moments of P3DDFT. **d**, After thermal annealing.

CFT could function as a charge-separation centre to generate photocurrent. Device fabrication using this method was highly reproducible: the standard deviation of each parameter was small, even though fabrication was conducted in air and water was used to dissolve the sacrificial layer. It is also noteworthy that a mixed bulk heterojunction (BHJ) film consisting of P3HT:PCBM could be transferred onto an ITO/poly(3,4-ethylenedioxythiophene):poly(*p*-styrene sulphonate) (PEDOT:PSS)/P3HT substrate for the fabrication of OPV devices (ITO/PEDOT:PSS/P3HT//P3HT:PCBM/Al). The performance of this device was comparable to that of conventional BHJ devices fabricated by spin-coating (details of the methods for device fabrication, the J–V characteristics and the performance of these devices are provided in the Supplementary Information). This result indicates that the CFT method can produce interfaces across which charge transport is as effective as across spin-coated interfaces.

Before the transfer, both the PCBM and P3HT surfaces were confirmed by atomic force microscopy to be very flat (typical arithmetic roughness (R_a) values are 0.39 nm and 0.27 nm, respectively). Insofar as the conditions of the CFT method are mild (no pressure, heat or organic solvent), the interface of the PCBM//P3HT bilayer can be expected to retain a degree of flatness similar to that of the PCBM and P3HT surfaces. The performance, especially the J_{SC} value, of PCBM//P3HT bilayer OPVs fabricated in the present study was lower in comparison with OPVs fabricated by other methods that have been previously reported. PCBM/P3HT bilayer OPVs were fabricated by a poly(dimethylsiloxane) stamping method[10], and a PCE of 0.97% was reported with a J_{SC} of 6.4 mA cm^{-2}. PCBM/P3HT bilayer OPVs fabricated by spin-coating using orthogonal solvents (that is, solvents that do not dissolve the organic layer underneath) were also reported[19], giving a PCE of 1.4% with a high J_{SC} of 6.1 mA cm^{-2}. The former method requires both heat and external pressure to transfer the polymer film, and the latter is a solution-based process. Therefore, in the case of these two methods, it is possible that there is intermixing of the materials at the interface, which would produce a local BHJ-like structure contributing to the higher J_{SC}. Recently, it has been reported that residual vapour of organic solvents can induce substantial intermixing of materials at a laminated interface[13,14]. In contrast, the CFT method should produce a well-defined PCBM//P3HT interface without intermixing of the materials. In addition, because the surface of the spin-coated P3HT film is covered with aligned and ordered alkyl side chains, as suggested by previous research[18], a single sheet of the alkyl chain layer divides the fullerene part and the polythiophene backbone. This could decrease the likelihood of charge separation in comparison with thermally annealed or spin-coated interfaces that would have less ordered alkyl structures.

To support the formation of the well-defined bilayer structure by the CFT method, X-ray reflectivity measurements were carried out on the PCBM//P3HT films. The successful fit to the bilayer model and the agreement on the thicknesses indicate that the PCBM//P3HT interface is well defined as expected from the mild conditions of the CFT method (see Supplementary Information).

Next, we modified the surface properties of both PCBM and P3HT films with SSMs to modulate the OPV characteristics. We have already proposed the concept of an SSM that spontaneously forms on an organic semiconductor film[20–22]. Because fluoroalkylated compounds have low surface energy, these molecules segregate on the film surface as a monolayer during spin-coating of a mixture solution. We have shown previously that the fluoroalkylated fullerene ([6,6]-phenyl-C_{61}-butyric acid 1H,1H-perfluoro-1-nonyl ester (FC_8) in Fig. 2c) forms an SSM during spin-coating from a mixture solution of PCBM and FC_8, and induces alignment of the molecular dipole moments of fluoroalkyl chains on the surface[22]. In this work, we expanded the application of SSMs to include those made of polymer materials. A poly(3-alkylthiophene) derivative with fluoroalkyl

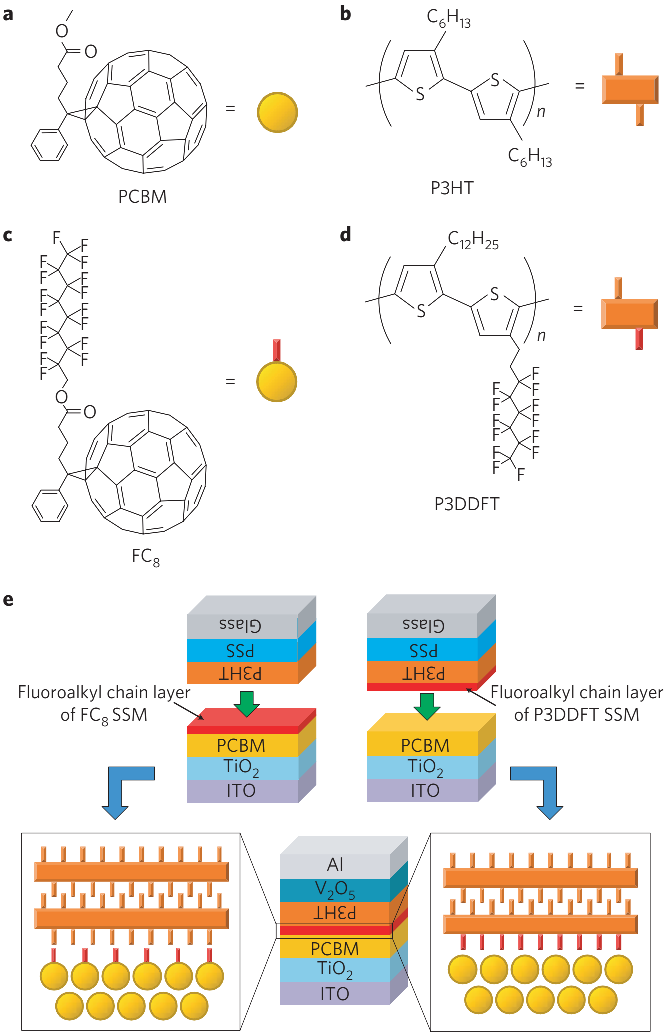

Figure 2 | Chemical structures of the materials used and schematic representations of the insertion of the SSM. a, PCBM. **b**, P3HT. **c**, FC_8. **d**, P3DDFT. **e**, Insertion of the FC_8 or P3DDFT SSM by the CFT method and models of the interface structures.

side chains (poly(4′-dodecyl-3-[1H,1H,2H,2H-perfluorooctyl]-2,2′-bithiophene)s (P3DDFT) in Fig. 2d) was synthesized and used as an SSM in combination with P3HT. X-ray photoelectron spectroscopy (XPS) analysis of the P3HT/P3DDFT mixed films showed that the surface had a high F/C atom ratio compared with that in solution (Table 2), suggesting the surface segregation of P3DDFT. When the concentration of P3DDFT was increased in the mixture solution, the fluorine signal was clearly observed to saturate, which is similar to the case of FC_8 SSM. In addition, the depth profile by XPS showed that P3DDFT was present only on the surface of the film and no F peak was observed in the bulk of the film. From these results, we concluded that, because of the alternative side-chain substituents, P3DDFT formed a dense SSM on the P3HT film surface with the orientation of the polythiophene backbone similar to that of P3HT. Details of the synthesis and the SSM formation of P3DDFT will be reported elsewhere (Y. F. Geng, Q. S. Wei, K. Tajima, & K. Hashimoto, manuscript in preparation).

Four types of film, namely PCBM, PCBM/FC_8, P3HT and P3HT/P3DDFT, were prepared by spin-coating, and the ionization potentials (IPs) of the films were measured by UPS. The results are shown in Fig. 4 and Table 2. The IP values calculated from the spectral width are summarized in Table 2. From these results, we can clearly see the shift of IP when the FC_8 or P3DDFT was mixed in the PCBM or P3HT solution, respectively. The IP of the PCBM film was shifted from 5.87 to 6.14 eV with the FC_8 SSM on the surface. This difference of +0.27 eV was consistent with the previously reported result[22]. Moreover, the IP of the P3HT film with the P3DDFT SSM on the surface was 5.47 eV, which was much larger than that of the pristine P3HT film (4.29 eV). This increase in IP demonstrated that the fluoroalkyl chains of P3DDFT formed the SSM with dipole moments on the P3HT film. Here, a +1.18 eV shift of the IP was reached. This larger shift compared with the case of the PCBM/FC_8 film can be attributed to the higher density of the dipole moments, because the fluoroalkyl side chains of P3DDFT can be packed more densely than those of FC_8, as deduced from the molecular structures. This is supported by the fact that the F/C atom ratio on the surface of the P3HT/P3DDFT film was much larger than that of the PCBM/FC_8 film (Table 2). Cyclic voltammetry measurements showed that FC_8 has the same first reduction potential as PCBM (ref. 22), suggesting that the IP shifts observed by UPS are not due to changes in the energy levels of the semiconducting part caused by fluoroalkyl substitution, but rather due to the dipole moments formed on the surface. On the other hand, the oxidation onset potential of the P3DDFT film (+0.56 V versus Fc/Fc^+) was different from that of the P3HT film (+0.39 V versus Fc/Fc^+), indicating that changes in the level of the HOMO could contribute to the increase in IP. However, compared with this difference (+0.17 V), the shift of the vacuum level at the surface estimated from the shift of the cutoff in the UPS spectrum was much larger; therefore, the increase in IP was mainly due to the dipole moments formed on the surface. On the basis of these results, we can conclude that fluoroalkyl chains of the SSM induced the dipole moments on each surface of the PCBM and P3HT films.

Combining these two findings, we next fabricated bilayer OPV devices with organic semiconductor films with an SSM inserted at the donor/acceptor interface. The structures of the devices were ITO/TiO_2/PCBM/FC_8//P3HT/V_2O_5/Al and ITO/TiO_2/PCBM//P3DDFT/P3HT/V_2O_5/Al. The PCBM/FC_8 and P3DDFT/P3HT layers were 40 and 50 nm in thickness, respectively. Note that the surfaces of the donor and acceptor were characterized before junction formation. This means that the FC_8 SSM or the P3DDFT SSM with dipole moments was inserted between the P3HT and PCBM layers as schematically shown in Fig. 2e, and the choice of SSM (FC_8 or P3DDFT) can change the direction of the interfacial dipole moments. The J–V characteristics of these two devices are shown in Fig. 3a. The PCBM/FC_8//P3HT device exhibited a V_{OC} of 0.31 ± 0.02 V (Table 1). Compared with the V_{OC} of the PCBM//P3HT device, the V_{OC} of the PCBM/FC_8//P3HT device was smaller by 0.19 V. This decrease of V_{OC} is consistent with the direction of the interfacial dipole moments of the FC_8 SSM, which decreases ΔE_{HL} at the interface as shown in Fig. 1b. In contrast, the PCBM//P3DDFT/P3HT device exhibited a V_{OC} of 0.86 ± 0.04 V (Table 1). The V_{OC} was up to 0.36 V greater than that of the PCBM//P3HT device. The direction of the change of the V_{OC} is opposite to that of the PCBM/FC_8//P3HT device, and is consistent with the hypothesis that the interfacial dipole moments of the P3DDFT SSM increase ΔE_{HL} (Fig. 1c). Note here that this bilayer device showed quite high V_{OC} for the combination of P3HT and PCBM in an OPV, which typically gives a V_{OC} of 0.5–0.7 V (refs 10, 19,23,24), including bilayer and BHJ-type devices, depending on the fabrication conditions. The best value we achieved was 0.95 V, which is the highest V_{OC} reported for the combination of P3HT and PCBM.

To confirm that the alignment of the interfacial dipole moments of the SSM actually contributed to the change of V_{OC}, we thermally annealed the three types of bilayer device at 120 °C for 5 min after

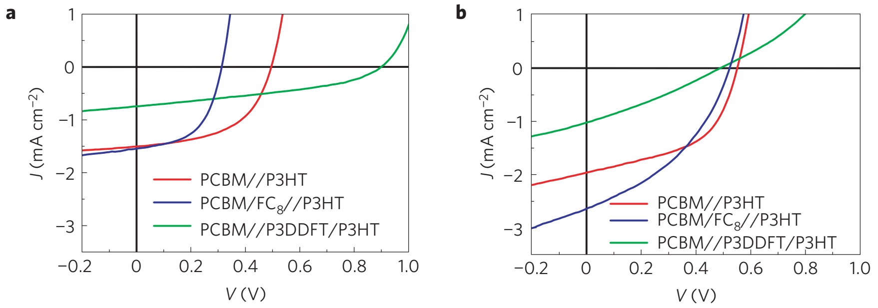

Figure 3 | *J*–*V* characteristics under 100 mW cm^{-2}, AM1.5 irradiation of three types of bilayer device fabricated by the CFT method. a, As prepared. **b**, Annealed at 120 °C for 5 min.

Table 1 | Summary of the OPV performance of three types of bilayer device fabricated by the CFT method (as prepared and annealed at 120 °C for 5 min).

		V_{OC} (V)	J_{SC} (mA cm^{-2})	FF (—)	PCE (%)
PCBM//P3HT	As prepared	0.50 (0.03)	1.51 (0.11)	0.53 (0.06)	0.40 (0.07)
	Annealed	0.55 (0.01)	1.88 (0.08)	0.48 (0.02)	0.50 (0.04)
PCBM/FC$_8$//P3HT	As prepared	0.31 (0.02)	1.51 (0.06)	0.50 (0.03)	0.23 (0.03)
	Annealed	0.52 (0.03)	2.65 (0.04)	0.44 (0.05)	0.60 (0.08)
PCBM//P3DDFT/P3HT	As prepared	0.86 (0.04)	0.70 (0.07)	0.38 (0.02)	0.23 (0.03)
	Annealed	0.51 (0.05)	1.15 (0.12)	0.32 (0.04)	0.19 (0.06)

Values inside parentheses are standard deviations.

the deposition of the metal electrodes. Recently, several groups have reported that the thermal annealing of bilayer OPV devices induced significant intermixing of the two layers[25–30]. We also confirmed this intermixing by X-ray reflectivity and XPS depth-profile measurements on the bilayer structures prepared by the CFT method (see Supplementary Information).

The *J*–*V* characteristics of the annealed devices are shown in Fig. 3b, and the results are summarized in Table 1. The V_{OC} values of the three annealed devices clearly converged to similar values around 0.5 V after the thermal annealing. This value was almost the same as that of the as-prepared PCBM//P3HT device. The film analyses and the device characterizations indicated that the intermixing induced by the thermal annealing leads to the randomizing of the aligned dipole moments and the disappearance of the electric fields at the interfaces (Fig. 1d). Moreover, the thermal annealing improved J_{SC} for all three devices in comparison with the as-prepared devices, suggesting that the area of the charge separation interface increased owing to the intermixing of the two layers. From these results, we can conclude that the aligned dipole moments at the interfaces play a key role in the observed V_{OC} shifts.

It might be argued that the fluoroalkyl compounds might exist elsewhere than the organic/organic interfaces, which could change the device properties. To clarify this point, the films of PCBM/FC$_8$ and P3HT/P3DDFT were transferred by the CFT method upside down onto the substrates and the presence of F atoms on the surfaces was analysed by XPS. As a result, very small F 1s signals in the XPS spectra were observed; the F/C atom ratios are 0.0054 and 0.0043 for FC$_8$/PCBM and P3DDFT/P3HT, respectively. These results indicate that there are small amounts of the fluorinated compounds trapped at the substrate/organic interface during the spin-coating and these compounds could remain at the organic/electrode interfaces in the OPV devices. However, such low levels of F atoms on the surface induce very little IP shift and therefore the differences at the organic/electrode interfaces have negligible effects on the large difference of V_{OC} observed here. XPS depth profiles on PCBM/FC$_8$ and P3HT/P3DDFT films showed that F signals were observed only at the surface and no signal was detected in the bulk of the films.

We also fabricated bilayer devices with the 'normal' OPV structures of ITO/PEDOT:PSS/P3HT/C$_{60}$/Ca/Al and ITO/PEDOT:PSS/P3HT/P3DDFT/C$_{60}$/Ca/Al by spin-coating the polymer layers and subsequently vacuum depositing C$_{60}$, Ca and Al on the top. As a result, by the insertion of the dipole moment of the surface-segregated P3DDFT layer, we observed the change of V_{OC} by +0.4 V, which is similar to that of the inverted structures prepared by the CFT method (see Supplementary Information). These results further support the idea that the observed shift of V_{OC} is not related to the stacking order of the layers or the device structure, but due to the effect of the dipole moments at the donor/acceptor interface.

For both FC$_8$ and P3DDFT, the V_{OC} shifts were smaller than the values calculated from the IP shifts. Two reasons for this discrepancy are discussed as follows. The first reason is a change in the effective dielectric constant. As the UPS measurements were carried out under high vacuum, the energy-level shift was evaluated using the dielectric constant of vacuum. However, in the actual devices, dipole moments exist in the organic materials, so the shift of the energy levels could be decreased by the relative dielectric constant of these organic materials. The second reason is that V_{OC} depends not only on ΔE_{HL} but also on the orbital overlap between the HOMO of the donor and the LUMO of the acceptor. It has been reported that when this overlap decreased, the dark saturation current was reduced and the V_{OC} was decreased to a lesser extent[31]. The overlap between molecular orbitals possibly decreases owing to the fluoroalkyl chain layer of FC$_8$ or P3DDFT at the interface. Further quantitative analysis of the IP shift and V_{OC} change is now in progress.

Finally, we need to address the change of J_{SC} with the interfacial SSMs. Whereas the J_{SC} of the PCBM/FC$_8$//P3HT device was similar to that of the PCBM//P3HT device, the PCBM//P3DDFT/P3HT device showed significantly lower J_{SC}. This result is consistent with the external quantum efficiency spectra of the devices (see Supplementary Information). The existence of the fluoroalkyl

Table 2 | Summary of XPS and UPS results for the four types of organic film.

	F/C atom ratio in solution (—)*	F/C atom ratio on surface (—)†	Ionization potential (eV)‡
PCBM	0	0	5.87
PCBM/FC$_8$	0.015	0.094	6.14
P3HT	0	0	4.29
P3HT/P3DDFT	0.019	0.22	5.47

*Calculated from the molar concentration of each material. †Measured by XPS. ‡Measured by UPS.

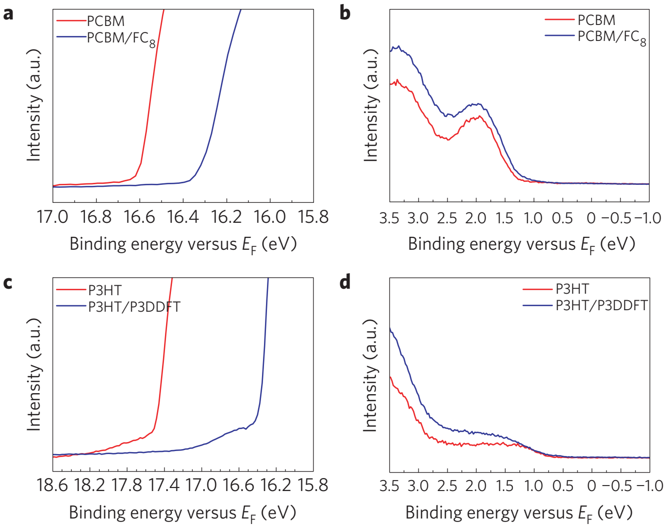

Figure 4 | UPS spectra for the four types of film using He(I) irradiation. **a**,**b**, PCBM and PCBM/FC$_8$. **c**,**d**, P3HT and P3HT/P3DDFT. **a**,**c**, Cutoff. **b**,**d**, Fermi-edge regions. The *x* axis shows the binding energy relative to the Fermi level of each material.

SSM at the interface should also affect the offset of the LUMO energies, which is the driving force for the charge separation. At the same time, it could change the donor–acceptor distance at the interface, which is related to the electronic coupling. Therefore, the larger drop of J_{SC} in the PCBM//P3DDFT/P3HT device might be qualitatively explained by the decreases of the LUMO–LUMO offset and the increase of the distance between P3HT and PCBM due to the existence of the P3DDFT SSM. In the case of the PCBM/FC$_8$//P3HT device, these two factors could work in opposing directions for the charge separation (that is, a larger LUMO offset but a longer donor–acceptor distance), so such a simple explanation is not possible. In fact, there are a multitude of factors involved in photocurrent generation, such as the absorption and the roughness at the interface. It is therefore difficult to make a quantitative analysis of the J_{SC} changes at this stage, and further investigations are necessary. In particular, it could be interesting to see the critical point at which the photoelectron transfer shuts down by bringing the LUMO levels even closer.

In conclusion, we have shown that, by inserting aligned dipole moments at the interface between organic donor and acceptor layers, ΔE_{HL} was shifted according to the direction of the dipole moments, which resulted in the change of the V_{OC} from 0.3 to 0.95 V, even for the same combination of the bulk materials. Although it is still necessary to establish a model that can explain the device behaviour quantitatively, this methodology could provide an experimental approach to obtaining fundamental information on the photoinduced charge-separation process at organic heterointerfaces, such as the effects of the energy levels, electronic coupling and molecular orientations[32]. The current findings might be also applicable to BHJ-like structures if well-defined large molecular interfaces and distinctly separated charge-transport paths could be constructed in the films.

Methods

The inverted bilayer device with the structure ITO/TiO$_2$/PCBM (Frontier Carbon, Japan)//P3HT (Rieke Metals, USA)/V$_2$O$_5$/Al was fabricated as follows. ITO-coated glass substrates (sheet resistance $10\,\Omega^{-1}$, Geomatech) were cleaned by ultrasonication in detergent, water, acetone, 2-propanol and water again for 30 min, and were exposed to ultraviolet–ozone for 20 min. TiO$_2$ precursor solution (NDH-510C, Nippon Soda) diluted by ethanol was spin-coated on the ITO substrates at a spinning rate of 3,000 r.p.m. for 30 s followed by drying at 140 °C for 40 min and calcination at 500 °C for 30 min to form an electron-transporting layer. Then, the substrates were again cleaned by ultrasonication in acetone and 2-propanol, and chlorobenzene solution containing $10\,\mathrm{g\,l^{-1}}$ of PCBM was spin-coated onto the ITO/TiO$_2$ substrates at a spinning rate of 600 r.p.m. for 60 s. The substrates were thermally annealed at 150 °C for 5 min inside a N$_2$-filled glove box. The substrates with the structure glass/PSS (Aldrich)/P3HT were prepared by successive spin-coatings. PSS was a sacrificial layer and was prepared by spin-coating of aqueous solution containing $10\,\mathrm{g\,l^{-1}}$ of PSS at a spinning rate of 4,000 r.p.m. for 30 s on the glass substrates, which were precleaned and exposed to ultraviolet–ozone in the same way as were the ITO substrates. Chlorobenzene solution containing $10\,\mathrm{g\,l^{-1}}$ of P3HT was spin-coated on the glass/PSS substrates at a spinning rate of 1,000 r.p.m. for 60 s. Then, the glass/PSS/P3HT substrate was gently placed, upside down, onto the ITO/TiO$_2$/PCBM substrate, and one drop of water was placed on the edge of the two substrates. Water selectively penetrated and dissolved the PSS layer, and as a result the P3HT layer was transferred onto the PCBM layer. A V$_2$O$_5$ hole-transporting layer (4 nm) and Al electrodes (50 nm) were deposited by thermal evaporation under high vacuum ($\sim 10^{-4}$ Pa) in a vacuum evaporation system (H-2807 vacuum evaporation system with E-100 load lock, ALS Technology, Japan). The fabricated devices were characterized as prepared or after thermal annealing at 120 °C for 5 min in a glove box for the experiment on interfacial mixing (see main text).

Two other inverted bilayer devices were fabricated in a similar manner. The device with the structure ITO/TiO$_2$/PCBM/FC$_8$//P3HT/V$_2$O$_5$/Al was fabricated as described above, but chlorobenzene solution containing $10\,\mathrm{g\,l^{-1}}$ of PCBM and $1.0\,\mathrm{g\,l^{-1}}$ of FC$_8$ was used. The device with the structure ITO/TiO$_2$/PCBM//P3DDFT/P3HT/V$_2$O$_5$/Al was also fabricated as described above, but hot chlorobenzene solution (120 °C) containing $5.0\,\mathrm{g\,l^{-1}}$ of P3HT and $0.50\,\mathrm{g\,l^{-1}}$ of P3DDFT was used.

The J–V characteristics of the OPV devices were measured using a J–V measurement system (Keithley 2400) under AM1.5 simulated solar light irradiation (PEC-L11, Peccell Technologies). The active area of the devices was defined by a photomask as $0.12\,\mathrm{cm^2}$. The light intensity was adjusted to $100\,\mathrm{mW\,cm^{-2}}$ by a standard silicon solar cell (BS520, Bunkou Keiki, Japan).

The film thicknesses were measured by using surface profilometry (Dektak 6M, ULVAC, Japan). XPS and UPS were carried out on an AXIS-ULTRA DLD spectrometer (Kratos Analytical). X-ray photoelectron spectra were obtained by using Al Kα radiation. Ultraviolet photoelectron spectra were obtained with He(I) excitation of 21.2 eV and a pass energy of 5 eV. For all UPS analyses, a bias of 6 V was applied to the substrates.

Received 30 September 2010; accepted 12 April 2011;

References

1. Ishii, H., Sugiyama, K., Ito, E. & Seki, K. Energy level alignment and interfacial electronic structures at organic metal and organic organic interfaces. *Adv. Mater.* **11,** 605–625 (1999).
2. Zhu, X. Y. & Kahn, A. Electronic structure and dynamics at organic donor/acceptor interfaces. *MRS Bull.* **35,** 443–448 (2010).
3. Gregg, B. A. & Hanna, M. C. Comparing organic to inorganic photovoltaic cells: Theory, experiment, and simulation. *J. Appl. Phys.* **93,** 3605–3614 (2003).

4. Scharber, M. C. *et al.* Design rules for donors in bulk-heterojunction solar cells—towards 10% energy-conversion efficiency. *Adv. Mater.* **18,** 789–794 (2006).
5. Rand, B. P., Burk, D. P. & Forrest, S. R. Offset energies at organic semiconductor heterojunctions and their influence on the open-circuit voltage of thin-film solar cells. *Phys. Rev. B* **75,** 115327–115337 (2007).
6. Gadisa, A., Svensson, M., Andersson, M. R. & Inganäs, O. Correlation between oxidation potential and open-circuit voltage of composite solar cells based on blends of polythiophenes/fullerene derivative. *Appl. Phys. Lett.* **84,** 1609–1611 (2004).
7. Potscavage, W. J., Sharma, A. & Kippelen, B. Critical interfaces in organic solar cells and their influence on the open-circuit voltage. *Acc. Chem. Res.* **42,** 1758–1767 (2009).
8. Yim, K. H. *et al.* Efficient conjugated-polymer optoelectronic devices fabricated by thin-film transfer-printing technique. *Adv. Funct. Mater.* **18,** 1012–1019 (2008).
9. Chen, L. C., Degenaar, P. & Bradley, D. D. C. Polymer transfer printing: Application to layer coating, pattern definition, and diode dark current blocking. *Adv. Mater.* **20,** 1679–1683 (2008).
10. Huang, J. H. *et al.* Fabrication of multilayer organic solar cells through a stamping technique. *J. Mater. Chem.* **19,** 4077–4080 (2009).
11. Nakamura, M., Yang, C. H., Tajima, K. & Hashimoto, K. High-performance polymer photovoltaic devices with inverted structure prepared by thermal lamination. *Sol. Energy Mater. Sol. Cells* **93,** 1681–1684 (2009).
12. Nakamura, M., Yang, C. H., Zhou, E. J., Tajima, K. & Hashimoto, K. Polymer bulk heterojunction photovoltaic devices with multilayer structures prepared by thermal lamination. *ACS Appl. Mater. Interfaces* **1,** 2703–2706 (2009).
13. Wang, D. H. *et al.* Unexpected solid–solid intermixing in a bilayer of poly(3-hexylthiophene) and 6,6-phenyl $C_6$1-butyric acidmethyl ester via stamping transfer. *Org. Electron.* **11,** 1376–1380 (2010).
14. Wang, D. H., Choi, D. G., Lee, K. J., Park, O. O. & Park, J. H. Photovoltaic devices with an active layer from a stamping transfer technique: Single layer versus double layer. *Langmuir* **26,** 9584–9588 (2010).
15. Wei, Q. S., Tajima, K. & Hashimoto, K. Bilayer ambipolar organic thin-film transistors and inverters prepared by the contact-film-transfer method. *ACS Appl. Mater. Interfaces* **1,** 1865–1868 (2009).
16. Wei, Q. S., Miyanishi, S., Tajima, K. & Hashimoto, K. Enhanced charge transport in polymer thin-film transistors prepared by contact film transfer method. *ACS Appl. Mater. Interfaces* **1,** 2660–2666 (2009).
17. Wei, Q. S., Tajima, K. & Hashimoto, K. Electrical instability of polymer thin-film transistors using contact film transfer methods. *Appl. Phys. Lett.* **96,** 243301–243303 (2010).
18. Hao, X. T. *et al.* Control of the interchain π–π interaction and electron density distribution at the surface of conjugated poly(3-hexylthiophene) thin films. *J. Phys. Chem. B* **111,** 10365–10372 (2007).
19. Ayzner, A. L., Tassone, C. J., Tolbert, S. H. & Schwartz, B. J. Reappraising the need for bulk heterojunctions in polymer–fullerene photovoltaics: The role of carrier transport in all-solution-processed P3HT/PCBM bilayer solar cells. *J. Phys. Chem. C* **113,** 20050–20060 (2009).
20. Wei, Q. S., Nishizawa, T., Tajima, K. & Hashimoto, K. Self-organized buffer layers in organic solar cells. *Adv. Mater.* **20,** 2211–2216 (2008).
21. Yamakawa, S., Tajima, K. & Hashimoto, K. Buffer layer formation in organic photovoltaic cells by self-organization of poly(dimethylsiloxane)s. *Org. Electron.* **10,** 511–514 (2009).
22. Wei, Q. S., Tajima, K., Tong, Y. J., Ye, S. & Hashimoto, K. Surface-segregated monolayers: A new type of ordered monolayer for surface modification of organic semiconductors. *J. Am. Chem. Soc.* **131,** 17597–17604 (2009).
23. Li, G. *et al.* High-efficiency solution processable polymer photovoltaic cells by self-organization of polymer blends. *Nature Mater.* **4,** 864–868 (2005).
24. Kim, S. S., Na, S. I., Jo, J., Tae, G. & Kim, D. Y. Efficient polymer solar cells fabricated by simple brush painting. *Adv. Mater.* **19,** 4410–4415 (2007).
25. Ferenczi, T. A. M. *et al.* Planar heterojunction organic photovoltaic diodes via a novel stamp transfer process. *J. Phys.: Condens. Matter* **20,** 8 (2008).
26. Collins, B. A. *et al.* Molecular miscibility of polymer–fullerene blends. *J. Phys. Chem. Lett.* **1,** 3160–3166 (2010).
27. Yan, H. *et al.* Influence of annealing and interfacial roughness on the performance of bilayer donor/acceptor polymer photovoltaic devices. *Adv. Funct. Mater.* **20,** 4329–4337 (2010).
28. Treat, N. D. *et al.* Interdiffusion of PCBM and P3HT reveals miscibility in a photovoltaically active blend. *Adv. Energy Mater.* **1,** 82–89 (2011).
29. Chen, D. A., Nakahara, A., Wei, D. G., Nordlund, D. & Russell, T. P. P3HT/PCBM bulk heterojunction organic photovoltaics: Correlating efficiency and morphology. *Nano Lett.* **11,** 561–567 (2011).
30. Lee, K. H. *et al.* Morphology of all-solution-processed 'bilayer' organic solar cells. *Adv. Mater.* **23,** 766–770 (2011).
31. Perez, M. D., Borek, C., Forrest, S. R. & Thompson, M. E. Molecular and morphological influences on the open circuit voltages of organic photovoltaic devices. *J. Am. Chem. Soc.* **131,** 9281–9286 (2009).
32. Duhm, S. *et al.* Orientation-dependent ionization energies and interface dipoles in ordered molecular assemblies. *Nature Mater.* **7,** 326–332 (2008).

Acknowledgements

Y.F.G. thanks the Chinese Scholarship Council for financial support.

Author contributions

A.T. and Y.F.G. contributed equally to this work. A.T. fabricated and evaluated the OPV devices and carried out the external quantum efficiency, XPS, UPS and X-ray reflectivity measurements. Y.F.G. synthesized and characterized the P3DDFT and carried out the XPS depth profile measurements. Q.S.W. synthesized and characterized the FC_8. K.H. and K.T. directed the research. A.T., K.H. and K.T. wrote the paper.

Additional information

The authors declare no competing financial interests. Supplementary information accompanies this paper on www.nature.com/naturematerials. Reprints and permissions information is available online at http://www.nature.com/reprints. Correspondence and requests for materials should be addressed to K.H. or K.T.